THIS IS AN EARLY ACCESS ARTICLE.
This article has been accepted for publication in a future issue of this journal,
but has not been fully edited. Content may change prior to final publication.

BULLETIN OF THE POLISH ACADEMY OF SCIENCES
TECHNICAL SCIENCES
DOI: 10.24425/bpasts.2027.6292

Deflection assessment of a shell embedded in soil under applied load: a case study

Czesław Machelski[1], Zofia Zięba[1], Matylda Tankiewicz[1*], Mariusz Myszor[2]

[1] Wrocław University of Environmental and Life Sciences, Department of Civil Engineering, Wrocław, Poland
[2] Wrocław University of Science and Technology, Faculty of Civil Engineering, Wrocław, Poland

Abstract. Displacement tests under live loads are most commonly used to determine the stiffness of soil-shell structures. However, for design purposes, it is also important to be able to determine the stiffness of a structure on the basis of theoretical models. This paper presents the results of a comparative analysis of various methods for determining the deflection influence surface of a shell. Results of tests on real structures were compared with calculations from an elastic half-space model and a simplified 3D numerical model. Both the longitudinal and transverse profiles of the structure were analyzed. Based on the achieved results, it was concluded that Boussinesq's solution did not account for the structure's geometry or its different behavior in different directions. In the case of numerical analysis, however, even a simplified model yields results close to the actual ones and may help estimate the stiffness of a structure. The study also analyzes the influence of cover depth and load distribution on deflection profiles. It was found that as the thickness of cover depth increased, the deflection at the crown decreased. These results may prove useful for determining load distribution in complex automotive wheel systems.

Key words: soil-shell structure; soil-steel bridge; live loads; cover depth

1. INTRODUCTION

Soil-shell structures are bridges made of arched shells embedded in the ground [1-2]. They are widely used as an alternative to traditional engineering solutions, characterized by lower material consumption, ease of construction, and lower implementation costs [1]. Shell, typically made of corrugated sheet, is characterized by very low stiffness and strength. The bearing capacity of the structure results from the interaction between the shell and the compacted soil backfill [3-6]. The stiffness of the structure depends not only on the type, shape, and stiffness of the shell, but also on the type of backfill used and the method of its placement, including the thickness of the layer above the shell crown. In the initial stage of shell covering, the sides of the shell are pushed inwards, while its crown is raised. Subsequently, as the height of the backfill increases, the upper part of the shell moves downwards. When subjected to vehicle traffic, the soil-steel structure undergoes deformation, which depends not only on the type and magnitude of the load, but also on the load's position and the direction of a movement [2].

Due to the complex nature of soil-shell structures, they are still the subject of research and analysis [7-20]. Numerous studies available in the literature mainly concern the analysis of the behavior of real structures [17, 20], model studies [9, 12, 16], and numerical modelling [7, 8, 11, 13, 15] in various conditions. In practice, the stiffness of bridge structures is determined based on the results of tests conducted under live loads [21]. From the results of measurements of structural displacements when the position of the vehicle along the road centerline changes, a deflection function is determined [22]. In complex structural systems, the deflection influence surface is mapped on this basis. However, for design purposes, it is also important to be able to determine the stiffness of a structure based on theoretical models. Due to its construction, a soil-shell structure will have different stiffness along the longitudinal and transverse axes. In the case of such constructions, the correct determination of the influence surface is extremely important for the safety of the structure due to the high susceptibility of the shell itself and the interaction between the cover and the shell [8, 23].

The paper presents a verification of simple computational models used to assess the influence surface based on results from real objects. Unlike advanced methods, they are characterized by their ease of use and do not require costly and time-consuming examinations. The work considers the load situation after the completion of the structure without pavement and the initial operation of the finished structure with pavement. Both the longitudinal and transverse profiles of the deflection influence surface were analyzed. The results from tests on real structures were compared with calculations obtained from a half-space elastic model (Boussinesq's solution) and a simplified 3D numerical model, reduced to the influence surface. The results shown, that Boussinesq's solution does not allow for the correct assessment of the behavior in both directions due to the variable geometry of the structure, but even a simple numerical model allowed for results close to the

*e-mail: matylda.tankiewicz@upwr.edu.pl

This article has been accepted for publication in a future issue of this journal, but has not been fully edited. Content may change prior to final publication.

actual ones. The analysis also took into account the varying depth of soil cover above the shell crown in order to assess the impact of the load. The results presented may be also useful in estimating the load distribution in complex vehicle wheel systems.

2. LOAD INFLUENCE ON THE SHELL

In the past, Boussinesq's solution [24] was used to assess the efficiency of complex vehicle load systems. According to this theory normal stress σ(x,y) directed at given depth z may be treated as a distributed force p(x,y) with a direction normal to the shell surface. Normal force p(x,y) and tangential force t(x,y) are contact interactions between the soil and the shell. In the modeling of soil-shell structures, they are treated as a static condition of cooperation between the two different elements [25]. The condition of reciprocal displacements in the radial direction is also fulfilled.

If we consider the load of a concentrated force P located on the ground level, normal stress at given depth in the z axis direction is given by the formula:

$$\sigma(x,y) = \frac{3Pz^3}{2\pi r^5}. \qquad (1)$$

where the distance between the point of application of the force and the point under consideration on the shell is expressed by the radius r:

$$r = \sqrt{x^2 + y^2 + z^2}. \qquad (2)$$

The shell crown marked as point K lies directly below the origin of the coordinate system at a distance z, as shown in Fig. 1.

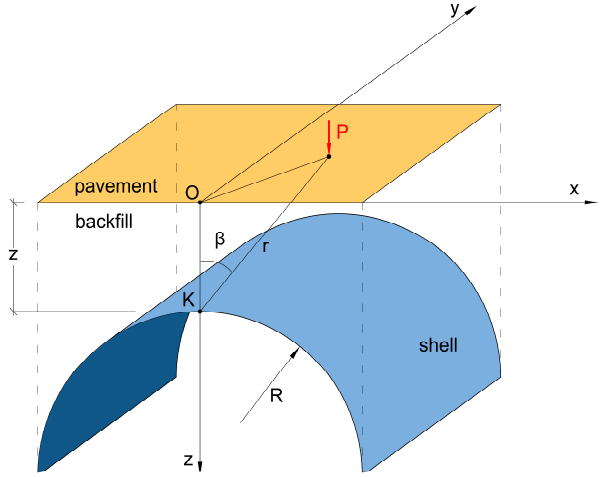


Fig.1. Diagram of the structure and P force loading on the ground level

In the special case where force P is located directly above the analyzed point of the shell K i.e. when r = z, the following is obtained:

$$\sigma_0 = \frac{3P}{2\pi z^2} \qquad (3)$$

A comparison of Eq. (1) and (3) results in a normalized function of the form:

$$B(x,y) = \frac{\sigma(x,y)}{\sigma_0} = \left(\frac{z}{r}\right)^5 \qquad (4)$$

where:

$$\frac{z}{r} = \left[\left(\frac{x}{z}\right)^2 + \left(\frac{y}{z}\right)^2 + 1\right]^{-1/2} = cos\beta \qquad (5)$$

The function B(x,y), with the value of 1 when x = y = 0, together with the constant factor as in formula (1), is the load influence surface of point K with the general form:

$$p(x,y) = \frac{3P}{2\pi z^2} B(x,y) \qquad (6)$$

When considering the change in the position of force P relative to point O (and K), a cross-sectional profile B(y) obtained along the y axis, and when the change in position of the force concerns the x axis, a longitudinal profile B(x) is obtained. From the form of Eq. (2) and (4) it can be seen that both profiles are identical and were designated as B in the paper.

3. DEFLECTION INFLUENCE SURFACE AND PROFILES OF THE SHELL CROWN

When analyzing the deflection of the shell crown from the applied force P located on the ground plane, the influence surface in the form of the function η(x,y) [26] is used. According to the definition of the influence surface, for any position of force P the deflection of the shell crown is obtained as:

$$w_k = P \cdot \eta(x,y) \qquad (7)$$

where x and y are the coordinates of the point of application of force P on the structure's ground level, in relation to the crown (point K) and point O. In the special case where force P is located directly above point K we obtain:

$$w_k = P \cdot \eta_k \qquad (8)$$

By comparing formulas (7) and (8), the normalized function of the deflection influence surface of the crown can be determined:

$$A(x,y) = \frac{\eta(x,y)}{\eta_k} \qquad (9)$$

With a value of 1 at the origin of the coordinate system, when x = y = 0. Due to the method of determination, it is analogous to the function B(x,y), given in Eq. (4).

When the load is the group of m identical forces, in the case of a motor vehicle, the following formula is obtained:

$$w_k = P \cdot \sum_{j=1}^{m} \eta(x_j, y_j) \qquad (10)$$

and taking into account A(x,y) from Eq. (9), the following function is obtained:

$$w_k = P \cdot \eta_k \sum_{j=1}^{m} A(x_j, y_j) \qquad (11)$$

In the further part of the paper, the function A(x,y) in the longitudinal and transverse sections is described as A(x) and A(y), respectively. Both profiles have a common maximum ordinate η_k.

In the case of bridge structures, motor vehicles travel along the road centerline, i.e., the x axis. In the general case, when the line of wheels is located along the x axis (the direction of travel), and the other is offset by y = b (wheelbase on the axle), Eq. (10) gives the deflection of the shell crown in the form of two components with the following values:

$$w_k = \sum_{i=1}^{n} P_i \cdot \eta(a_i, 0) + \sum_{i=1}^{n} P_i \cdot \eta(a_i, b) \qquad (12)$$

where n is the number of axles in the vehicle. In the formula, Pi is assumed as the wheel pressure in the longitudinal spacing ai. The maximum deflection value occurs when one of the wheel lines is located above the shell crown:

$$w_k = [1 + A(b)] \cdot \sum_{i=1}^{n} P_i \cdot \eta(a_i) \qquad (13)$$

Eq. (13) takes into account the cross-sectional profile A(y=b) of the influence surface η(x,y). When equal wheel load values Pi are assumed and the longitudinal profile A(x) of the

This article has been accepted for publication in a future issue of this journal, but has not been fully edited. Content may change prior to final publication.

deflection influence surface from Eq. (13) the following is obtained:

$$w_k = P \cdot \eta_k \cdot [1 + A(b)] \cdot \sum_{i=1}^{n} A(a_i) \quad (14)$$

When the maximum value of w_k occurs, the center axis of the vehicle is located above the crown, and therefore the ordinate is $\eta(x,y) = \eta_k$. Thus, Eq. (14) takes on a special form as:

$$w_k = P \cdot \eta_k \cdot [1 + A(b)] \cdot \sum_{i=2}^{n} [1 + A(a_i)] (15)$$

The stiffness [21] and inertia with damping of bridges are of significant importance for their dynamics. The stiffness is calculated on the basis of the maximum ordinate of the deflection influence surface η_k as in the formula:

$$k = \frac{1}{\eta_k} \quad (16)$$

In the analyzed soil-shell structures, the cover depth above the shell crown has a significant impact on the result. A higher value of z (see Fig.1) reduces deflection and thus increases the stiffness of the structure.

Soil-steel bridges are treated as compliant [27], i.e. with lower stiffness than classic short-span bridges. The compliance of a bridge is related to the stiffness of the longitudinal profile of the shell crown deflection influence surface A(x):

$$f = 2\eta_k \int_0^{x_0} A(x)dx \quad (17)$$

where the symmetry of the A(x) function is used in multiplier 2. When determining this function on the basis of test results using motor vehicles, the cross-sectional profile of the shell crown deflection surface A(y) is used, as in Eq. (15).

In the case of railway structures, Eq. (15) is modified when the measurement point is on the track axis, to the following form:

$$w_k = 2P \cdot \eta_k \frac{2}{b} \int_0^{b/2} A(y)dy \cdot \sum_{i=2}^{n} [1 + A(a_i)] (18)$$

where 2P is the pressure on the train axle, and a_i are the distances of the axles from the reference point. Dimension b takes into account the railway sleeper and ballast. Therefore, the value of z is calculated from the level of the backfill and not in relation to the position of force P on the ground (and road surface).

4. APPLICATION OF BOUSSINESQ'S SOLUTION

First, the deflection influence surfaces derived from Boussinesq's solution were analyzed. For this purpose, the results of acceptance tests of the bridge in Jeleniów [26] were used. Characteristic dimensions of the structure are: spanning length L = 5.66 m, height H = 1,46 m and radius of curvature R = 8.0 m. The shell was made of MP 1500×50×6 sheet metal. The geometry of the corrugated sheet shell is described by its technical designation a×f×t as a type with the following parameters: a – wave length, f – wave height, t – sheet thickness. The position of the vehicle was taken as the center axis of the vehicle, i.e., for x = 0. The tests used a Kamaz vehicle with rear axle loads of 2P3 = 73.0 kN and 2P2 = 76.8 kN and front axle load of 2P1 = 46.2 kN. The distances between the axles were a32 =1.32 m and a21 =2.85 m. The structure was characterized by a very low structural height above the crown (pavement with subgrade and backfill), only 0.5 m. Usually, this height is greater than 0.75 m.

Figure 2 shows two profiles of the shell crown deflection influence surface: longitudinal A(x) and transverse A(y), obtained as results of deflection measurement w(x,y) of the soil-shell structure. Function A(x) relates to the direction of vehicle travel, hence its tendency to tend to zero as the value of x increases. Therefore, it is natural that there is no deflection when the load is outside the bridge. In the study of the A(x) function, the vehicle assumed successive positions spaced apart by half the rear axle spacing, i.e. every 0.66 m. In this case, the shell diagram and its geometry as well as the type of corrugated sheet are taken into account. In the case of the A(y) function, there is a limitation in the form of the bridge width, in this case y < 3.8 m. Function A(y) was determined only from two vehicle settings in the cross-section of the roadway shifted by 1.8 m. Therefore, the shape of the structure indicates that the A(y) graph is an estimate. The limited reduction of the A(y) ordinates results from the same shape of the shell along the entire length of the culvert structure. Hence, the y line passing through the crown is a straight line, and the shell axis in the x direction changes according to the radius R, as shown in Fig. 1.

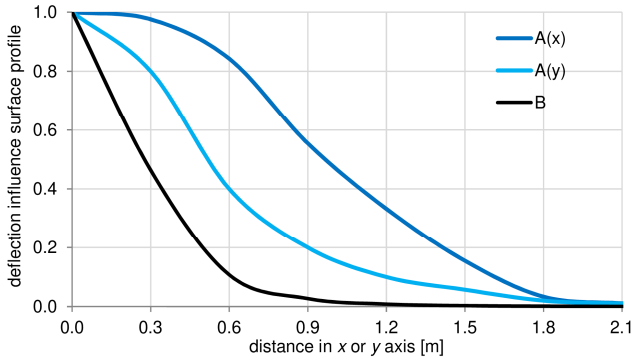


Fig.2. Profiles of the deflection surface of the structure in Jeleniów based on acceptance tests A(x) and A(y) and Boussinesq's solution B

The load influence surface, marked as B, was created based on completely different assumptions. In this case, the half-space of the soil medium is considered without taking into account the shell structure. Therefore, naturally, both forms of the B(x) and B(y) functions are identical and, by definition, asymptotically tend to zero (at infinity). In calculations B for the analyzed object, a layer of homogeneous soil with a thickness of 0.5 m was assumed above the key. Therefore, the actual structure of the bridge is not taken into account in the model.

The common element is the treatment of the functions A(x), A(y) and B as surface influence profiles when the load is a unit force P, moving along the ground, as in Fig. 1. The graphs of functions A(x) and A(y) demonstrate a different impact of the car wheels on the shell in various directions, completely dissimilar than in the impact model B, particularly in the x direction.

5. APPLICATION OF NUMERICAL MODEL

For the numerical analysis, a structure on the Niemcza bypass was selected [28]. It was built as a temporary bridge on the Wrocław – Kudowa road. The characteristic dimensions of the structure are spanning length L = 5.25 m, height H = 1.85 m and radius of curvature R = 2.75 m. In this case, exceptionally, the shell was made of flat sheet metal with a thickness of t =

This article has been accepted for publication in a future issue of this journal, but has not been fully edited. Content may change prior to final publication.

23 mm. The foundation of the shell on steel profiles was also unique.

The numerical analysis was performed using the finite element method in ZSoil 2018 v 18.12. The structure model, shown in Fig. 3, consisted of a steel shell embedded in the soil medium. The geometry of the model was selected based on the technical documentation of the analyzed object. The soil backfill was assumed to be a continuous, elastic medium with a Poisson's ratio ν = 0.25 and Young's modulus E = 80 MPa. Due to the type of sheet used in the construction the shell of the structure was modeled as isotropic. An elastic model with the following parameters was also adopted for steel: Young's modulus E = 205 GPa and Poisson's ratio ν = 0.3. In accordance with limitations analogous to those for the structure in Jeleniów, the limitations of the ground level dimensions in the model to a 10×10 m rectangle were taken into account.

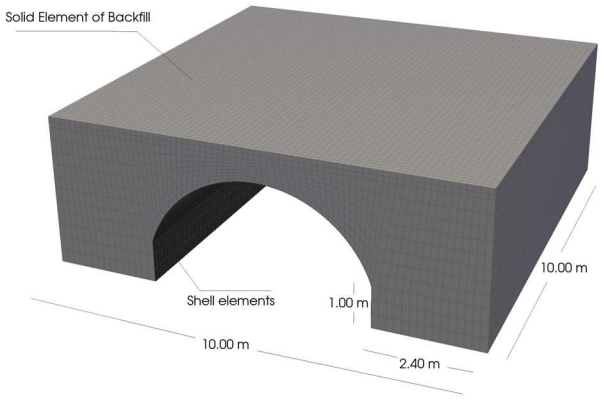


Fig.3. Visualization of the numerical model

When using calculations and a 3D object model to determine the deflection influence surface of the shell crown η(x,y), kinematic method is used [29]. Therefore, the vertical displacements of the ground surface w(x,y) = η(x,y) are treated as an influence function when the load is a unit force. Since the determination of the influence area and its subsequent use is based on the principle of superposition, this necessitates the use of elastic material models in the analyzed numerical model. The principle of superposition, which is the basis of many analytical methods, assumes the linearity of the system and the absence of material memory, which in practice means ignoring nonlinear phenomena and effects dependent on the load history. In reality, soil-shell structures exhibit strong hysteresis phenomena [13]. They result from both the compliance of the shell and the nonlinear contact between the shell and the soil. These phenomena have been confirmed both in experimental studies [30], and in numerical simulations [31, 32]. Thus, the use of simplified elastic models in the analyses of this type of structure becomes a necessity if the aim of the analysis is to maintain the principle of superposition.

The paper considers two operating modes of the structure: without pavement and with pavement. The calculation results are presented in the form of longitudinal profiles C(x) and transverse profiles C(y) of the deflection influence surface. They were normalized according to Eq. (4) so that they took the value 1 at point 0. The calculation results were related to the measurement results of the constructed structure marked as A and function B determined for the elastic half-space (as in Section 4).

Figure 4 displays the results for the structure under construction, without pavement, i.e., at z = 0.75 m. The tests were conducted using a Tatra truck with rear axle loads of 2P3 = 102 kN and 2P2 = 129 kN and a front axle load of 2P1 = 54 kN. The distances between the axles were a32 = 1.35 m and a21 = 3.55 m. When testing function A(x), the vehicle assumed successive positions spaced apart by half the rear axle spacing, i.e. every 0.675 m. The function A(y) was determined from a single position of the car in the cross-section of the road. In turn, Figure 5 compares the results of the constructed structure during acceptance tests, i.e. at z = 1.17 m. Function A(y) was determined on the basis of two positions of the car in the cross-section of the road, shifted by the wheelbase of the car, 1.8 m.

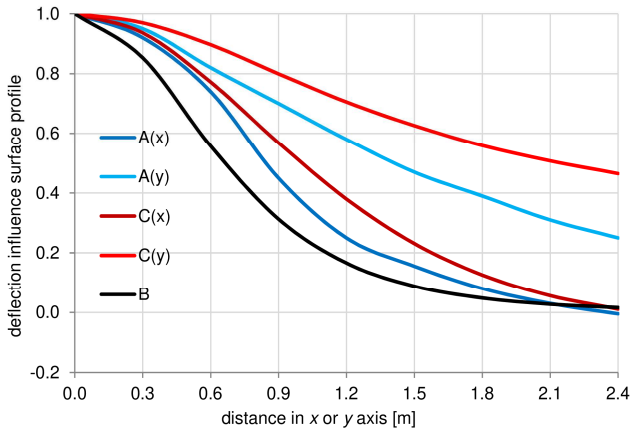


Fig.4. Deflection influence surface profiles of the structure in Niemcza without pavement (z=0.75m)

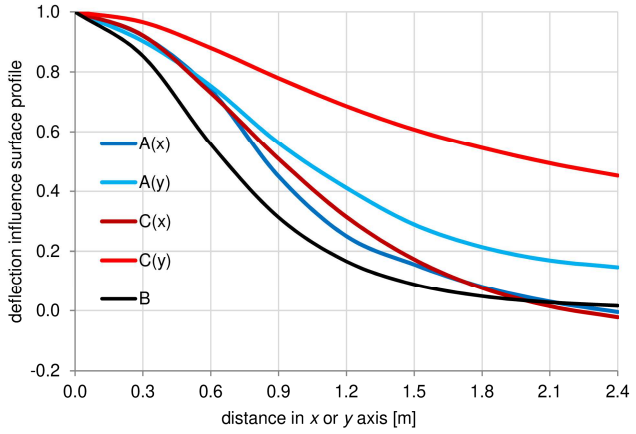


Fig.5. Deflection influence surface profiles of the finished structure in Niemcza (z=1.17m)

A comparison of functions A(x) and C(x) shows very good agreement of the results in the longitudinal section in both cases. A slightly larger difference for the variant with pavement may be caused by difficulties in modeling the upper layer of the roadbed, i.e., the pavement with subgrade [33]. The greater difference in the course of the transverse functions

This article has been accepted for publication in a future issue of this journal, but has not been fully edited. Content may change prior to final publication.

A(y) and C(y) may result from deviations of the model from the actual structure. In the structure, the shell is made of 1.5 m wide sheets, connected at points 1 m apart. In the model, the shell is a continuous surface. Additionally, it can be noted that the results from the numerical model are overestimated in relation to the experimental data, so using the values obtained from the numerical model is a safe approach. For larger structures, the proposed approach remains valid in principle; however, the numerical model should be adapted to the actual span, geometry and backfill conditions. The results marked as B again deviate significantly from the actual data, especially on the cross-section. Good agreement is only visible for the functions A(x) and B in the case of the structure with the pavement, but this is rather a coincidence.

6. ASSESSMENT OF THE INFLUENCE OF COVER DEPTH

In order to determine the influence of cover depth on the obtained deflection values, numerical calculations were performed again for the model described in point 5. The calculations were performed for four cover depths above the shell crown, i.e. 0.5, 0.75, 1.0, 1.25 m. The results of the calculations are presented in Figures 6 and 7 in the form of deflection influence surface profiles C(x) and C(y), as before. The analysis of the graphs shows significant differences in the transverse and longitudinal profiles and a change in the deflection profiles depending on the cover depth used. In addition, for the C(x) influence surface, an uplift of the ground surface is visible, which is also observed in reality.

Figure 8 additionally shows the load influence surface profiles B determined from the Boussinesq's solution, assuming a semi-elastic space. A very large difference is visible in comparison to the numerical model, in particular with regard to the transverse direction.

In practical applications, the distribution of loads on the wheels of a car is important. Road bridges are loaded by motor vehicles acting on the road surface through multiple wheels, as shown in Fig. 9a. In the case of small structures, the deflection profiles of the structure are affected by a set of double wheels with pressure P. Therefore, when there is one force P above the analyzed point K, it causes deflection, as in Eq. (8). Taking as a reference value the case for a layer thickness of z=0.75 m, the graphs shown in Fig. 9b are obtained as a function:

$$C1(z) = \frac{C(z)}{C(z=0{,}75)} \qquad (19)$$

In the case of a four-wheel system for diagram 9a, when one of them is above point K, the following is obtained from formula (15):

$$C4(z) = \frac{[1+C(1,8)]\cdot[1+C(1,32)]}{C(z=0{,}75)} \qquad (20)$$

where C(1,8) = C(y=b) and C(1,32) = C(x=a). These were obtained as the results of calculations from the model discussed earlier and the graphs shown in Fig. 6 and 7.

Graph C1 (in Fig. 9b) shows a clear reduction in the maximum deflection of the shell crown as the cover depth above the crown z increases. In the case of a motor vehicle, a corresponding function C4 is obtained. However, when the backfill value z>1, the deflection values from vehicle C4 stabilize at the level of deflection C1 from a single force at z = 0.75 m. This means that an increase in backfill height above a certain value does not result in an increase in the stiffness of the structure. On the other hand, when comparing the results for a single wheel (C1) and a set of wheels (C4), a relatively small increase in deflection, by approx. 30%, is visible in relation to the load of one wheel. This means that a single wheel located above the shell crown has a decisive influence on the deflection, and the contribution of the other three wheels of the car is much smaller.

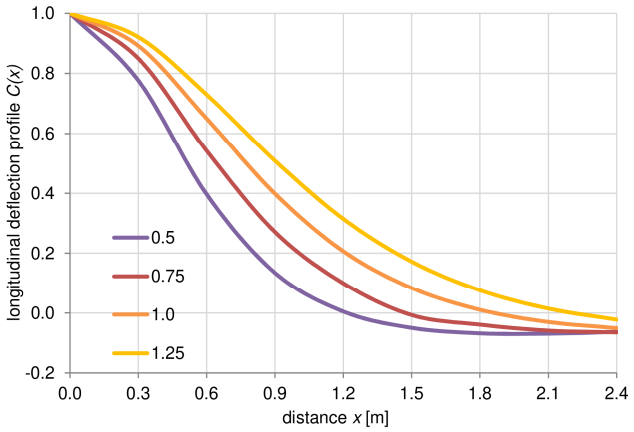


Fig.6. Longitudinal deflection profiles C(x) for different depths of the cover z based on a numerical model

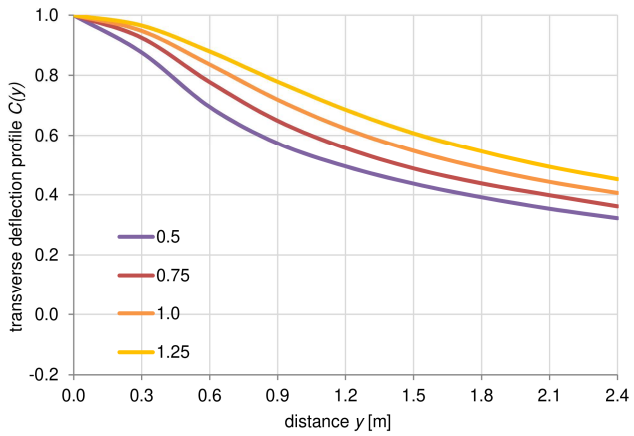


Fig.7. Transverse deflection profiles C(y) for different depths of the cover z based on a numerical model

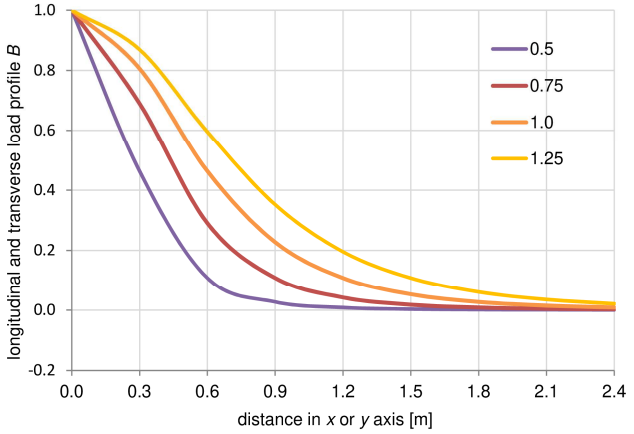


Fig.8. Longitudinal and transverse load profiles B for different depths of the cover z based on Boussinesq's solution

This article has been accepted for publication in a future issue of this journal, but has not been fully edited. Content may change prior to final publication.

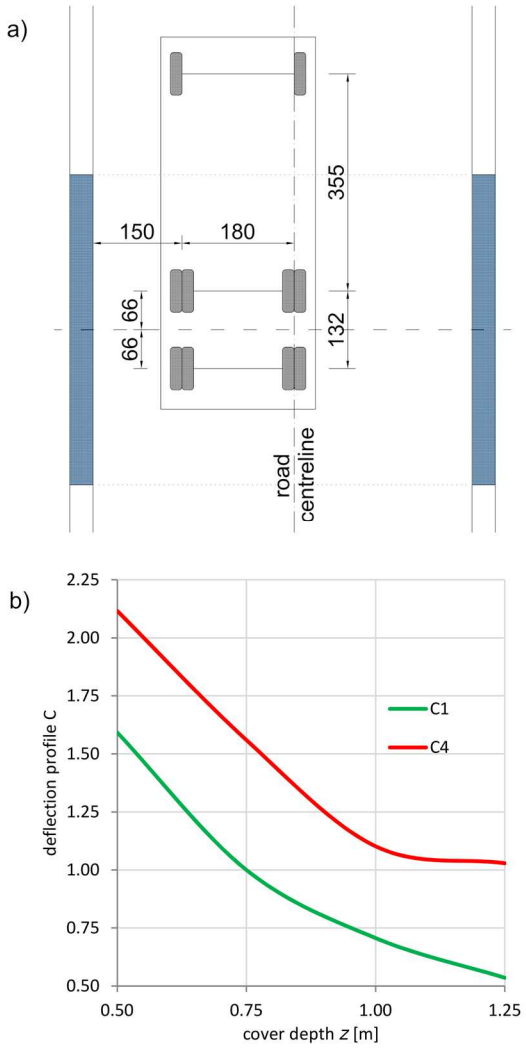


Fig.9. Cover depth influence on vehicle loads a) vehicle model b) deflection of the structure from a single wheel and a four-wheel system

7. CONCLUSIONS

The results discussed in this paper are the basis for determining the stiffness of bridge structures under operation. To determine the stiffness, it is necessary to obtain the maximum ordinate of the deflection influence surface. In the case of soil-shell structures, both the characteristics of the shell used (its shape and stiffness) and the physical properties of the soil backfill in its layered structure are of significant importance. The article presents a detailed comparative analysis of the test results of constructed structures with the results of calculations obtained from a half-space elastic model and a simplified 3D numerical model. These results were reduced to the deflection surface and, after normalization, longitudinal and transverse profiles were determined. The main conclusions are as follows:

- Direct measurements naturally take into account the actual characteristics of the structure (A), which are inevitably omitted in simplified models, however, it requires costly and time-consuming tests.
- The elastic half-space model (B), traditionally used in geotechnics, is easy to use, but does not provide satisfactory results in predicting the deflection of soil-shell structures, particularly in the longitudinal direction.
- Even with simplified numerical models (C) characteristics close to real ones can be obtained. Although they give overestimated values, can be used in preliminary analyses. Nevertheless, for more complex structures, the calculation time can be significant.
- The thickness of the layer above the shell crown is of significant importance for the stiffness and compliance of the object. A change in this thickness affects not only the maximum deflection of the shell, but also the nature of the deflection surface.
- In the case of complex load systems in the form of vehicle wheels, the contribution of individual forces determined on the basis of the shape of the impact surface function $\eta(x,y)$ is of additional importance. An essential feature of this algorithm is the correlation between the compliance of the structure and the stiffness of bridges as effects of stationary and live loads.

REFERENCES

[1] D. Beben, *Soil-Steel Bridges. Design, Maintenance and Durability*, Switzerland: Springer Nature, 2020.

[2] A.M. Legese, M. Sobótka, C. Machelski and A. Różański, "Behavior of soil-steel composite structure during construction and service: a review" *Arch. Civ. Eng.*, vol. 69, no. 4, pp. 263-292, 2023, doi: 10.24425/ace.2023.147659.

[3] D. Beben, "The role of backfill quality on corrugated steel plate culvert behaviour" *Baltic J. Road Bridge Eng.*, vol. 12, no. 1, pp. 1-11, 2017, doi: 10.3846/bjrbe.2017.01.

[4] H. El Naggar, A. Campbell and I. Ezzeldin, "Effect of the employed material model on the predicted behaviour of corrugated metal pipes" *Transp. Res. Rec.*, vol. 2675, no. 10, pp. 1364-1372, 2021, doi: 10.1177/03611981211016461.

[5] B. Liu, M. Zhang, P. Li and Z. Feng, "Effect of parameters on soil-structure interaction of a buried corrugated steel arch bridge", *Open Civ. Eng. J.*, vol. 5, pp. 154-162, 2011, doi: 10.2174/1874149501105010154.

[6] L. Pettersson and H. Sundquist, *Design of soil steel composite bridges,* Sweden: KTH Royal Institute of Technology, 2014.

[7] A. Elsawwaf, H. El Naggar and J. Newhook, "Effect of the employed soil constitutive model on the response of large-span soil steel bridges to soil and truck loading" *J. Constr. Steel Res.*, vol. 228, no. 109436, 2025, doi: 10.1016/j.jcsr.2025.109436.

[8] M. Esmaeili, J.A. Zakeri and P.H. Abdulrazagh, "Minimum depth of soil cover above long-span soil-steel railway bridges", *Int. J. Adv. Struct. Eng.*, vol. 5, pp. 1-17, 2013, doi: 10.1186/2008-6695-5-7

[9] K. Lang, M. Su, W. Shi, X. Ye, P. Yan, Z. Zhu, C. Zhang and J. Jin, "Nonlinear analysis of corrugated steel plate culverts using three-dimensional staged modelling under soil–steel interaction" *Structures*, vol. 79, no. 109480, 2025, doi: 10.1016/j.istruc.2025.109480.

[10] S. Mahjoubi and S. Maleki, „Finite element modelling and seismic behaviour of integral abutment bridges considering soil–structure interaction" *Eur. J. Environ. Civil Eng.*, vol. 24, no. 6, pp. 767-786, 2018, doi: 10.1080/19648189.2017.1421483.

[11] T. Maleska and D. Beben, "Behaviour of soil–steel composite bridges under strong seismic excitation with various boundary conditions" *Materials*, vol. 16, no. 2, 650, 2023, doi: 10.3390/ma16020650.

[12] I. D. Moore, C. Regier and N. A. Hoult, "Surface load testing of new circular and elliptical metal culverts at shallow cover" *Archiwum Instytutu Inżynierii Lądowej*, vol. 23, pp. 219-227, 2017, doi: 10.21008/j.1897-4007.2017.23.20.

[13] M. Sobótka and D. Łydżba, "Live load effect in soil-steel flexible culvert: role of apparent cohesion of backfill", *Eur. J. Environ. Civ. Eng.*, vol. 26, no. 2, pp. 620-634, 2019, doi: 10.1080/19648189.2019.1670264.

This article has been accepted for publication in a future issue of this journal, but has not been fully edited. Content may change prior to final publication.

[14] A. Rezaei and A. Derakhshani, "Fuzzy-stochastic stability analysis of soil-steel structures under uncertainty" *Multiscale Multidiscip. Model. Exp. Des.,* vol. 8, no. 1, 37, 2025, doi: 10.1007/s41939-024-00642-w.
[15] Wadi, L. Pettersson and R. Karoumi, "On predicting the ultimate capacity of a large-span soil–steel composite bridge", *Int. J. of Geosy. Ground Eng*., vol. 6, pp. 1-13, 2020, doi: 10.1007/s40891-020-00232-z.
[16] A. Wysokowski, "Full scale tests of various buried flexible structures under failure load" *Sci. Rep.*, vol. 12, no. 1, 1328, 2022, doi: 10.1038/s41598-022-04969-7.
[17] Y. Zhang, B. Liu, W. Sun and L. Meng, "Experimental and numerical study on longitudinal structural performance of soil-steel composite bridges", *Case Stud. Constr. Mater.*, vol. 22, e04148, 2025, doi: 10.1016/j.cscm.2024.e04148.
[18] X. Zheng, D.H. Yang, T.H. Yi and H.N. Li, "Bridge influence surface identification method considering the spatial effect of vehicle load" *Struct. Control Health Monit.*, vol. 28, no. 8, e2769, 2021, doi: 10.1002/stc.2769.
[19] X. Zheng, T.H. Yi, D.H. Yang, H.N. Li and Y. Zhou, "Bridge evaluation based on identified influence lines and influence surfaces: Multiple-scenario application" *Int. J. Struct. Stab. Dyn*., vol. 23, no. 16n18, 2340026, 2023, doi: 10.1142/S0219455423400266.
[20] X.Y. Zhou, M. Treacy, F. Schmidt, E. Brühwiler, F. Toutlemonde and B. Jacob, "Effect on bridge load effects of vehicle transverse in-lane position: A case study", *J. Bridge Eng*., vol. 20, no. 12, 04015020, 2015.
[21] O. Burdet and S. Corthay, "Static and dynamic load testing of Swiss Bridges" in: *International Bridge Conference Warsaw,* 1994.
[22] C. Machelski and M. Mumot, "Corrugated shell displacements during the passage of a vehicle along a soil-steel structure", Stud. Geotech. Mech., vol. 38, no. 4, pp. 25-32, 2016, doi: 10.1515/sgem-2016-0028.
[23] T. Maleska and D. Beben, "Numerical analysis of soil-steel bridge during backfilling using various shell models", *Eng. Struct.*, vol. 196, 109358, 2019.
[24] J. Boussinesq, "Application des potentiels a l'etude de l'equulibre et du mouvement des solid eselastiques", Gautier Villars, Paris, 1885.
[25] L. Pettersson, "Full scale tests and structural evaluation of soil steel flexible culverts with low height of cover" PhD thesis, KTH Royal Institute of Technology, Sweden, 2007.
[26] C. Machelski and G. Antoniszyn, "Influence of live loads on the soil-steel bridges", *Stud. Geotech. Mech*., vol. 26, no. 3-4, pp. 91-119, 2004.
[27] J. Vaslestad, B. Kunecki and T.H. Johansen, "Twenty one years pressure measurements on buried flexible steel structure" *Archiwum Instytutu Inżynierii Lądowej*, vol. 1/2007, pp. 233-244, 2007.
[28] A.M. Legese, "Numerical modeling of soil-steel composite structures behavior under ultimate loads" PhD thesis, Wrocław University of Science and Technology, Poland, 2024.
[29] C. Machelski, "Kinematic method for the determination of influence function of internal forces in the steel shell of soil-steel bridges", Stud. Geotech. Mech., vol. 32, no. 3, pp. 27- 40, 2010.
[30] C. Machelski, G. Antoniszyn and B. Michalski, "Live load effects on a soil-steel bridge founded on elastic supports", *Stud. Geotech. Mech*., vol. 28, no. 2-4, pp. 65-82, 2006.
[31] M. Sobótka, "Numerical simulation of hysteretic live load effect in a soil-steel bridge", *Stud. Geotech. Mech*., vol. 36, no. 1, pp. 103–109, 2014, doi:10.2478/sgem-2014-0012.
[32] M. Sobótka and C. Machelski, "Hysteretic live load effect in soil-steel structure", *Eng. Trans.,* vol. 64, no. 4, pp. 493-499, 2016.
[33] P. Mackiewicz, "Fatigue tests of bituminous mixtures with inclusion on initial cracks", *J. Mater. Civ. Engineering*, vol. 25, no. 1, pp. 140-147, 2013, doi:10.1061/(ASCE)MT.1943-5533.0000581

This article has been accepted for publication in a future issue of this journal, but has not been fully edited. Content may change prior to final publication.